

## Supplementary Information for “Water-induced formation of an alkali-ion dimer in cryptomelane nanorods”

Shaobo Cheng,<sup>a,¶</sup> Vidushi Sharma,<sup>b,c,¶</sup> Altug S. Poyraz,<sup>d,e</sup> Lijun Wu,<sup>a</sup> Xing Li,<sup>f</sup> Amy C. Marschilok,<sup>d,g,h</sup> Esther S. Takeuchi,<sup>d,g,h</sup> Kenneth J. Takeuchi,<sup>g,h</sup> Marivi Fernández-Serra<sup>b,c</sup> and Yimei Zhu<sup>a</sup>

Tunneled metal oxides such as  $\alpha$ -Mn<sub>8</sub>O<sub>16</sub> (hollandite) have proven to be compelling candidates for charge-storage materials in high-density batteries. In particular, the tunnels can support one-dimensional chains of K<sup>+</sup> ions (which act as structure-stabilizing dopants) and H<sub>2</sub>O molecules, as these chains are favored by strong H-bonds and electrostatic interactions. In this work, we examine the role of water molecules in enhancing the stability of K<sup>+</sup>-doped  $\alpha$ -Mn<sub>8</sub>O<sub>16</sub> (cryptomelane). The combined experimental and theoretical analyses show that for high enough concentrations of water and tunnel-ions, H<sub>2</sub>O displaces K<sup>+</sup> ions from their natural binding sites. This displacement becomes energetically favorable due to the formation of K<sub>2</sub><sup>+</sup> dimers, thereby modifying the stoichiometric charge of the system. These findings have potentially significant technological implications for the consideration of cryptomelane as a Li<sup>+</sup>/Na<sup>+</sup> battery electrode. Our work establishes the functional role of water in altering the energetics and structural properties of cryptomelane, an observation that has frequently been overlooked in previous studies.

<sup>a</sup> Department of Condensed Matter Physics and Materials Science, Brookhaven National Laboratory, Upton, NY 11973, USA.

<sup>b</sup> Department of Physics and Astronomy, Stony Brook University, Stony Brook, NY 11794-3800, USA. E-mail: maria.fernandez-serra@stonybrook.edu

<sup>c</sup> Institute for Advanced Computational Science, Stony Brook University, Stony Brook, NY, 11794, USA.

<sup>d</sup> Energy Sciences Directorate, Brookhaven National Laboratory, Upton, NY 11973, USA.

<sup>e</sup> Department of Chemistry and Biochemistry, Kennesaw State University, Kennesaw, GA 30144, USA.

<sup>f</sup> School of Physics and Microelectronics, Zhengzhou University, Daxue Road 75, Zhengzhou, 450052 China.

<sup>g</sup> Department of Chemistry, Stony Brook University, Stony Brook, NY 11794, USA.

<sup>h</sup> Department of Materials Science and Chemical Engineering, Stony Brook University, Stony Brook, NY 11794, USA.

¶ These authors contributed equally to this work.

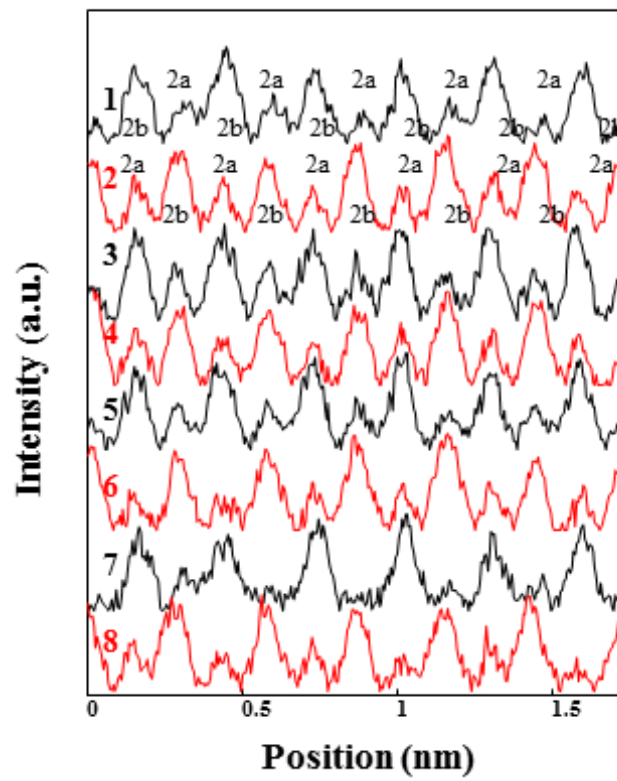


Fig. S1: Intensity profiles from eight vertical tunnels in Fig. 2b, showing intensity variation at '2a' sites. Note that the background has been subtracted for comparison.

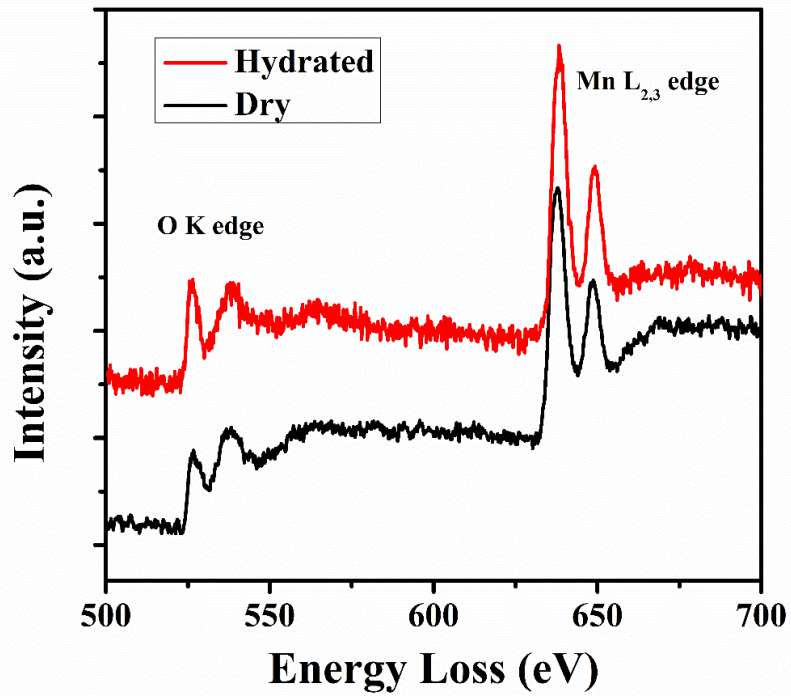


Fig. S2: Core loss electron energy-loss spectroscopy showing the dry and hydrated samples. The prepeak of O K edge in manganites reflects the concentration of oxygen in the materials. The prepeak from the hydrated sample is higher than that from the dry sample, indicating the presence of more water in the hydrated sample.

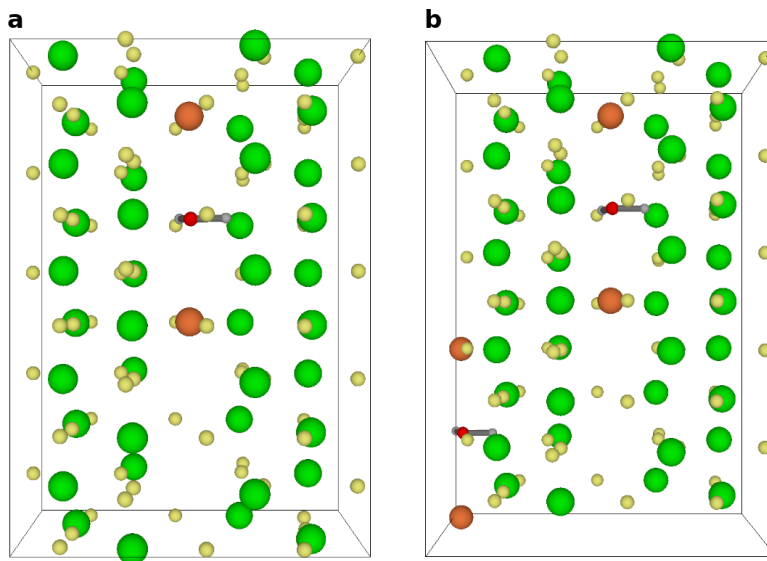


Fig. S3:  $K_{0.40}Mn_8O_{16} \cdot (0.20)H_2O$ : Two  $K^+$ 's and one  $H_2O$  occupying (a) one tunnel and, (b) both the tunnels of five unit cells of  $\alpha$ - $Mn_8O_{16}$ , shown along the  $a$ -axis. All atomic species occupy '2b' sites inside the tunnel(s). The binding energy of  $K^+$  is (a)  $-4.723$  eV and (b)  $-4.706$  eV.

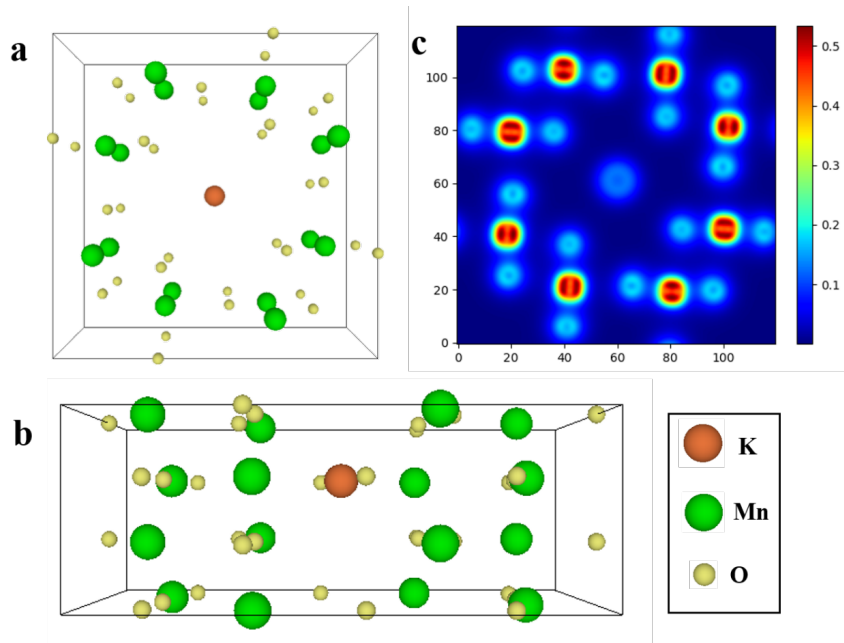


Fig. S4:  $K_{0.50}Mn_8O_{16}$ : K-doped two unit cells of  $\alpha$ - $Mn_8O_{16}$ , shown along (a) the  $c$ -axis, and (b) the  $a$ -axis.  $K^+$  attains a '2b' Wyckoff position inside the  $[2 \times 2]$  hollandite tunnel, surrounded by eight O's lying in the same plane as  $K^+$  itself. (c) Mean charge density plot of K-doped hollandite from the  $[001]$  axis showing  $K^+$  occupying the tunnel centered site. The binding energy of  $K^+$  ( $BE_K$ ) is computed to be  $-4.528$  eV.

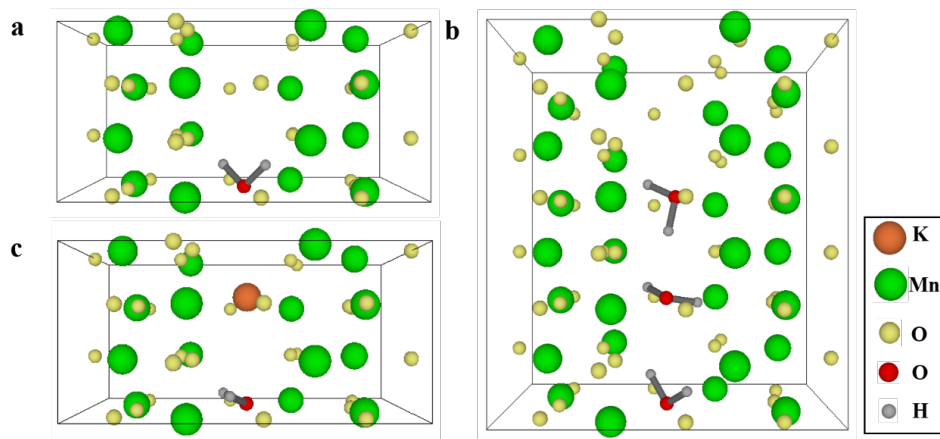


Fig. S5: DFT calculated results for hollandite cells containing water. (a)  $Mn_8O_{16} \cdot (0.50)H_2O$ .  $H_2O$  in two unit cells of  $\alpha$ - $Mn_8O_{16}$ , shown along the  $a$ -axis.  $H_2O$  attains a '2b' Wyckoff position inside the  $[2 \times 2]$  hollandite tunnel. The binding energy of  $H_2O$  is computed to be  $-0.212$  eV. (b)  $Mn_8O_{16} \cdot (0.75)H_2O$ . Three molecules of  $H_2O$  in four unit cells of  $\alpha$ - $Mn_8O_{16}$ , shown along the  $a$ -axis.  $H_2O$ 's attain '2b' Wyckoff positions inside the hollandite tunnel. The binding energy of  $H_2O$  is computed to be  $-0.475$  eV.  $H_2O$ 's form a H-bond chain spiraling down the axis of the tunnel (also the  $c$ -axis). (c)  $K_{0.50}Mn_8O_{16} \cdot (0.50)H_2O$ .  $K^+$  and  $H_2O$  in two unit cells of  $\alpha$ - $Mn_8O_{16}$ , shown along the  $a$ -axis.  $K^+$  and  $H_2O$  occupy '2b' Wyckoff positions inside the  $[2 \times 2]$  hollandite tunnel. The binding energy of K is  $-5.096$  eV; binding energy of  $H_2O$  is  $-0.772$  eV.

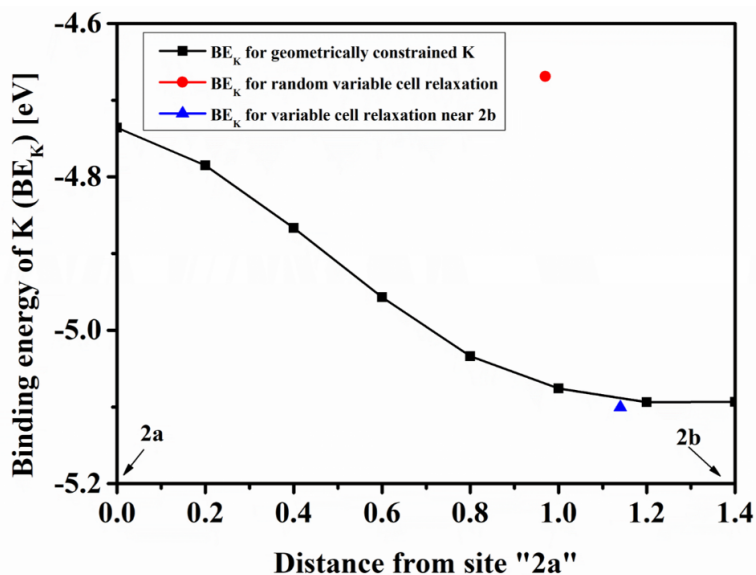


Fig. S6: Binding energy of  $K^+$  for constrained positions (from '2a' to '2b') of  $K^+$  inside the  $[2 \times 2]$  tunnel of  $K_{0.50}Mn_8O_{16} \cdot (0.5)H_2O$ . The black curve indicates the variation in the binding energy of  $K^+$  from a maximum at '2a' to a minimum at '2b', while water in the tunnel sits at '2b'. The blue point denotes the position attained by  $K^+$  under a variable cell-relaxation of the structure when the initial position of  $K^+$  is near '2b'. The red point represents a final position of  $K^+$  after a variable cell-relaxation when it was initially randomly placed, indicating the presence of several energy troughs along the tunnel axis.

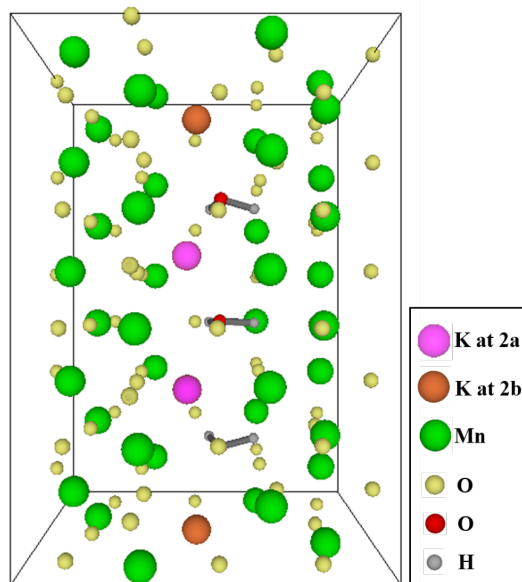


Fig. S7:  $K_{0.80}Mn_8O_{16} \cdot (0.60)H_2O$ : Four  $K^+$  and three  $H_2O$  in five unit cells of  $\alpha$ - $Mn_8O_{16}$ , shown along the a-axis. The two outer  $K^+$  ions occupy '2b' sites, and the two inner  $K^+$  ions are displaced by  $H_2O$ 's to occupy positions near '2a'. The  $H_2O$  trapped between  $K^+$  solvates it. The binding energy of  $K^+$  is  $-2.996$  eV. The higher binding energy accounts for the cost paid for overpopulating the tunnel.

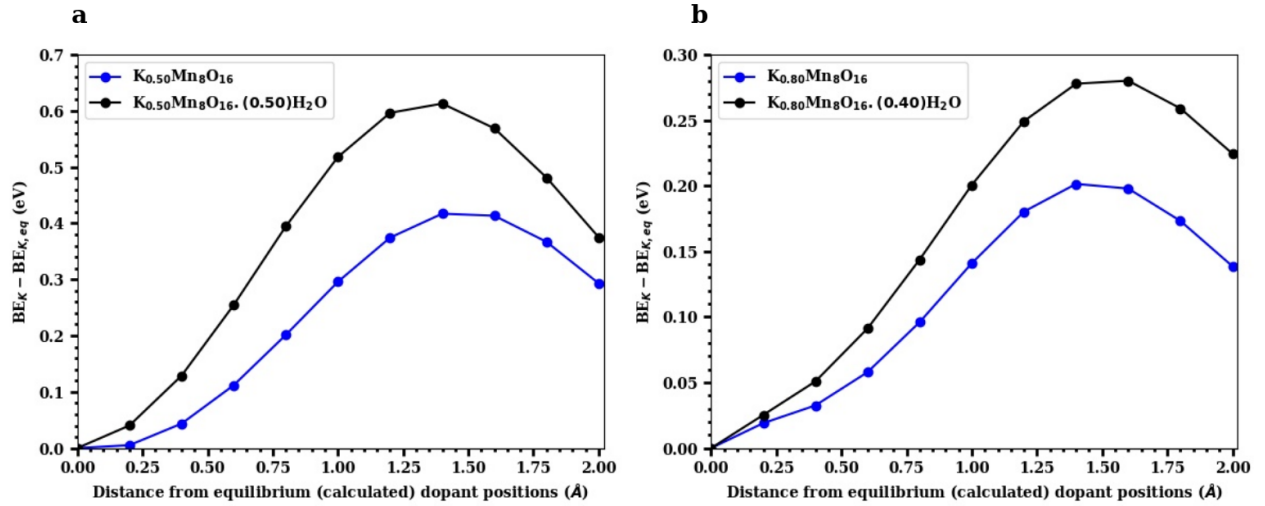


Fig. S8: Energetics of translating the dopants along the  $c$ -axis of the  $\alpha$ - $Mn_8O_{16}$  tunnel. The starting point is the equilibrium position of (all) dopants in the tunnel as obtained by our relaxation studies on the structures. The dopants are then uniformly shifted along the axis in intervals of 0.2 Å and the binding energy of potassium relative to that in the equilibrium position ( $BE_K - BE_{K,eq}$  [eV]) is computed for (a) low concentration of dopants with ( $K_{0.50}Mn_8O_{16} \cdot (0.50)H_2O$ ) and without water ( $K_{0.50}Mn_8O_{16}$ ), and (b) experimentally relevant - high concentration of dopants with ( $K_{0.80}Mn_8O_{16} \cdot (0.40)H_2O$ ) and without water ( $K_{0.80}Mn_8O_{16}$ ).

To illustrate the effect of  $H_2O$  on the movement of K along the tunnel, we estimate the energy barrier encountered by K both in the presence of water (black curve) and in its absence (blue curve) for two different concentrations of dopants as shown in Fig. S8:. The computed energy barriers are an upper bound to the actual barriers, because we do not conduct explicit barrier calculations. Instead we allow the entire system to relax, constraining the dopant position in the channel. In the low-dopant concentration regime Fig. S8:(a), the starting equilibrium configuration of dopants has K and  $H_2O$  situated at separate ‘2b’ sites and as we continue to move these dopants from their respective favorable positions, the binding energy of K continues to increase reaching its maximum where K and  $H_2O$  are both located at different ‘2a’ positions, yielding a barrier of  $\approx 0.42$  eV for the case with no water and  $\approx 0.60$  eV for the structure containing water. This seems to further suggest that the presence of water mostly stabilizes  $K^+$  at its original ‘2b’ position, making its departure from the equilibrium position less favorable. Furthermore, in the experimentally-relevant high concentration limit, Fig. S8:(b), the initial equilibrium dopant configuration now has K’s occupying a mix of ‘2b’ and ‘2a’ sites and translating all the dopants in the tunnel now results in a binding energy maximum where the K’s effectively exchange their ‘2b’ and ‘2a’ positions, with the inner K’s now at ‘2b’ and the outer ones at ‘2a’. The energy barrier for K in this densely occupied tunnel is  $\approx 0.20$  eV in the absence of water and  $\approx 0.28$  eV for water present in the tunnel. This is further evidence that though the presence of excess K’s improves the migration through the tunnel,  $H_2O$  still continues to stabilize the K’s by not lowering the energy barrier. Thus,  $H_2O$  does not facilitate the transport of K’s inside the  $\alpha$ - $Mn_8O_{16}$  tunnels, and tends to overall stabilize K’s in the originally chosen favorable coordination environment by forming a solvation shell around them.